ACS chemical biology

Articles

pubs.acs.org/acschemicalbiology

A Chemical Genetic Approach for Covalent Inhibition of Analogue-Sensitive Aurora Kinase

André Koch,[†,#] Haridas B. Rode,[‡,§,#] André Richters,[‡] Daniel Rauh,*[,‡,⊥] and Silke Hauf*[,†]

[†]Friedrich Miescher Laboratory of the Max Planck Society, Spemannstrasse 39, D-72076 Tübingen, Germany

[‡]Chemical Genomics Centre of the Max Planck Society, Otto-Hahn-Strasse 15, D-44227 Dortmund, Germany

[§]Council of Scientific and Industrial Research (CSIR) Headquarters, 2, Rafi Marg, New Delhi-110001, India

[⊥]Fakultät Chemie, Chemische Biologie, Technische Universität Dortmund, Otto-Hahn-Strasse 6, D-44227 Dortmund, Germany

Supporting Information

ABSTRACT: The perturbation of protein kinases with small organic molecules is a powerful approach to dissect kinase function in complex biological systems. Covalent kinase inhibitors that target thiols in the ATP binding pocket of the kinase domain proved to be ideal reagents for the investigation of highly dynamic cellular processes. However, due to the covalent inhibitors' possible off-target reactivities, it is required that the overall shape of the inhibitor as well as the intrinsic reactivity of the electrophile are precisely tuned to favor the reaction with only the desired cysteine. Here we report on the design and biological characterization of covalent anilinoquinazolines as potent inhibitors of genetically engineered Aurora kinase in fission yeast.

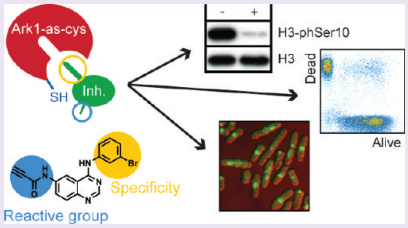

Protein kinases catalyze the transfer of phosphate groups from ATP to substrate proteins and are involved in nearly every signaling pathway.[1,2] A powerful approach used to unravel the complex nature of kinase biology is to perturb kinase function by small molecule inhibitors and to compare differences between perturbed and unperturbed states.[3] However, the limited selectivity of most inhibitors makes perturbation of a single kinase difficult.[4] Chemical genomics techniques such as the "bump-and-hole approach" allow for the acute chemical knock-down of target protein kinase function with precision and selectivity not possible with traditional genetic approaches.[5] Irreversible inhibitors are particularly powerful tools by covalently and thereby permanently perturbing kinase function at the cellular level and are moving to the forefront of kinase inhibitor research both in medicinal chemistry and chemical biology.[6] Compared to reversible inhibitors, such probes often remain bound throughout the lifetime of the target kinase, and the duration of their action is therefore a function of the rate of enzyme turnover.[7] Enhanced potency and efficacy of covalent kinase inhibitors may result in increased specificity and less susceptibility to ATP competitive effects, which often are bottlenecks in the development of specific kinase inhibitors.[6] Irreversible inhibitors can be designed to specifically target particular Cysteine (Cys) residues that are located in the vicinity of the ATP-binding pocket.[8,9] Cys797 in EGFR (epidermal growth factor receptor) continues to serve as a prototypic nucleophile for covalent kinase inhibition.[10] This Cys is located in a conserved α-helix at the lip of the ATP-binding pocket, which is naturally present only in a few eukaryotic kinases but can be introduced into other kinases of interest and be targeted by inhibitors carrying an electrophile.[11,12] The ideal covalent modifier is typically poorly reactive under physiological conditions with solution nucleophiles such as glutathione or solvent-exposed Cys and will react with the desired nucleophile only upon appropriate positioning within the binding pocket of the target kinase. In order to achieve this and to prevent the electrophile to indiscriminately form adducts with thiols of other proteins, it is necessary to tailor the reactivity of covalent inhibitors for the selected kinase. To further investigate the structural and chemical requirements for covalent inhibition of mutant kinase targets for chemical biology research, we set out to equip 4-anilinoquinazolines with various electrophiles, which complement for selectivity filters incorporated into the kinase domain of Aurora (Ark1) from fission yeast (*Schizosaccharomyces pombe*). The serine-threonine protein kinases of the Aurora family are essential for the proper execution of mitosis in eukaryotes.[13] The single Aurora in yeast (known as Ipl1 in budding yeast and Ark1 in fission yeast, in metazoans known as Aurora B) ensures that chromosomes become properly segregated by controlling chromosome compaction and chromosome attachment to the mitotic spindle, as well as cytokinesis and abscission.[14] We show that inhibition of Aurora in yeast is specific for the chosen selectivity filters in biochemical and cellular assays and is dependent on the nature of the selected electrophile.

Received: November 12, 2011
Accepted: January 20, 2012
Published: January 20, 2012

RESULTS AND DISCUSSION

Inhibitor and Mutant Kinase Design. We based the design of our probe molecules on a general kinase inhibitor scaffold that can be readily equipped with different electrophiles. The 4-anilinoquinazoline PD168393 (**1**) is one of the most studied covalent inhibitors of EGFR[15] and carries an acrylamide at the 6-position of the quinazoline core. In order to test for the electrophile best suited to inhibit mutant kinase activity, we selected propiolamide (**2**), *N*,*N*-dimethylamino-2-butenamide (**3**), and but-2-ynamide (**4**) as additional reactive groups (Figure 1A).

In order to develop a chemical genetic system for covalent inhibition of Aurora in fission yeast, we modified the ATP-binding site of Ark1 (i) to create analogue-sensitive (as) kinase alleles and (ii) to allow for covalent inhibition by 4-anilinoquinazolines. As a first selectivity filter, we exchanged leucine (Leu) 166, the gatekeeper residue in the hinge region of Ark1 (Figure 1B−D), to a smaller alanine residue in order to accommodate the bulky bromophenyl moiety of the inhibitors. Additional suppressor mutations, resulting in Ark1-as3, were needed to rescue the functionality of the kinase.[16] As a second selectivity filter glutamate (Glu) 173, located in a short helix following the hinge region of the kinase domain of Ark1 and isostructural to Cys797 in EGFR, was exchanged to Cys (Ark1-cys) (Figure 1B−D). We speculated that this Cys residue could serve as anchor point for covalent inhibition, thus further increasing compound specificity and potency.

Biochemical Validation of Inhibitors. We initially tested the inhibitory effect of **1**−**4** on recombinant Ark1 protein in various biochemical assays, and compared it to the outcomes seen with 1NM-PP1, a commonly used reversible ATP competitive inhibitor targeting gatekeeper-mutated analogue-sensitive kinase alleles.[17] As expected, 1NM-PP1 was able to inhibit Ark1-as3 and Ark1-as3-cys but did not have any effect on Ark1-cys or wild type Ark1 (Figure 2A, Supplementary Figure 1A). The IC_{50} for inhibition of Ark1-as3-cys was in the low nanomolar range (Figure 2B, Supplementary Table 1 and 2). In an end point assay using histone H3 as a substrate, compounds **1**−**4** were more efficient in inhibiting Ark1-as3-cys compared to Ark1-as3 and did not inhibit Ark1-cys (Figure 2A). The IC_{50} determinations showed that these molecules are potent, nanomolar inhibitors of Ark1-as3-cys, but not of Ark1 (Figure 2B, Supplementary Table 1). A reversible counterpart of **1** and **2** (**7**) inhibited Ark1-as3-cys with an IC_{50} considerably higher than that of **1** or **2** (272 ± 171 nM, Supplementary Table 1) and did not inhibit wild type Ark1, further highlighting that efficient inhibition by **1**−**4** may depend on covalent binding. In order to confirm that the engineered cysteine in Ark1-as3-cys can be covalently modified by the electrophilic compounds, we applied a fluorescence-based binding assay recently developed in our lab.[18] The assay exploits the fact that covalent bond formation of **1** and **3** with the introduced Cys173 in Ark1-as3-cys leads to an increase in fluorescence emission of the inhibitor. We observed fast covalent bond formation with Ark1-as3-cys but not with wild type Ark1 (Supplementary Figure 2). Covalent binding of **2** and **4** results in a different addition product when compared to **1** and **3** and leaves a double bond, which does not change fluorescence emission of the inhibitor. However, binding of **2** and **4** could be detected indirectly, since preincubation with these compounds blocked binding of **1** and **3** (Supplementary Figure 2B). To further analyze binding of **2** and **4**, we

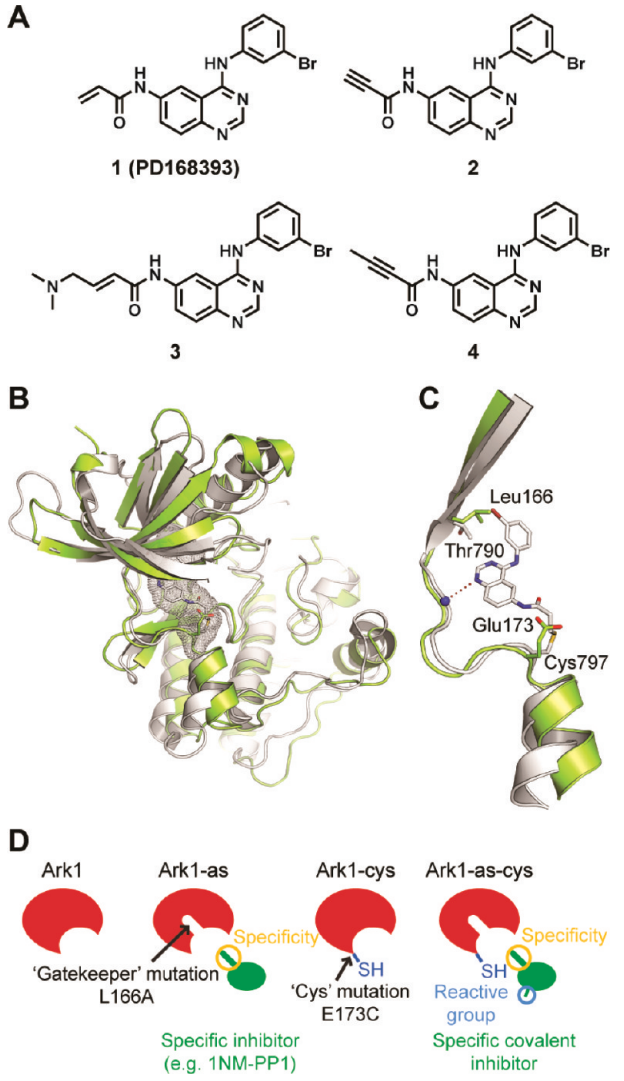

Figure 1. Covalent inhibitors and design of genetically engineered Ark1 kinase versions. (A) Chemical structures of compounds **1**−**4**. (B) Structural alignment of EGFR (gray) (in complex with the irreversible inhibitor **1**, PDB code: 2J5F) and a homology model of apo Ark1 from fission yeast (green) based on the crystal structure of *Xenopus* Aurora B (PDB code: 2BFY). (C) Detailed view of structural alignment highlighting the hinge region of the kinase domain with the gatekeeper position (Leu166, Thr790) and the short α-helix (Glu173, Cys797). Quinazoline-based inhibitors form key hydrogen bonds to the hinge region of the kinase domain (red dotted line). Cys797 of EGFR is covalently modified by **1**, and Glu173 in Ark1 is iso-structural to Cys797 in EGFR and was mutated to Cys to allow for covalent modification. The larger gatekeeper in Ark1 (Leu166) had to be replaced by a smaller amino acid to accommodate the bulky *m*-bromophenyl moiety of the inhibitor. (D) Schematic representation of wild type and mutant Ark1 kinase alleles. The Ark1-as version used in this study (Ark1-as3) has the additional mutations Q28R, Q176R, and S229A,[16] which rescue functionality of the kinase in which the gatekeeper is mutated (L166A).

derivatized these compounds by attaching the fluorophore BODIPY *via* a poly(ethylene glycol) linker to the 7-position of the quinazoline core to generate functional probes **5** and **6** (Figure 2C). Previous experiments had demonstrated that the 7-position of the quinazoline scaffold is likely to be solvent -exposed even after binding to the target kinase.[11,19] Probe **6** bound in an SDS-resistant and therefore covalent manner to

dx.doi.org/10.1021/cb200465c | *ACS Chem. Biol.* 2012, 7, 723−731

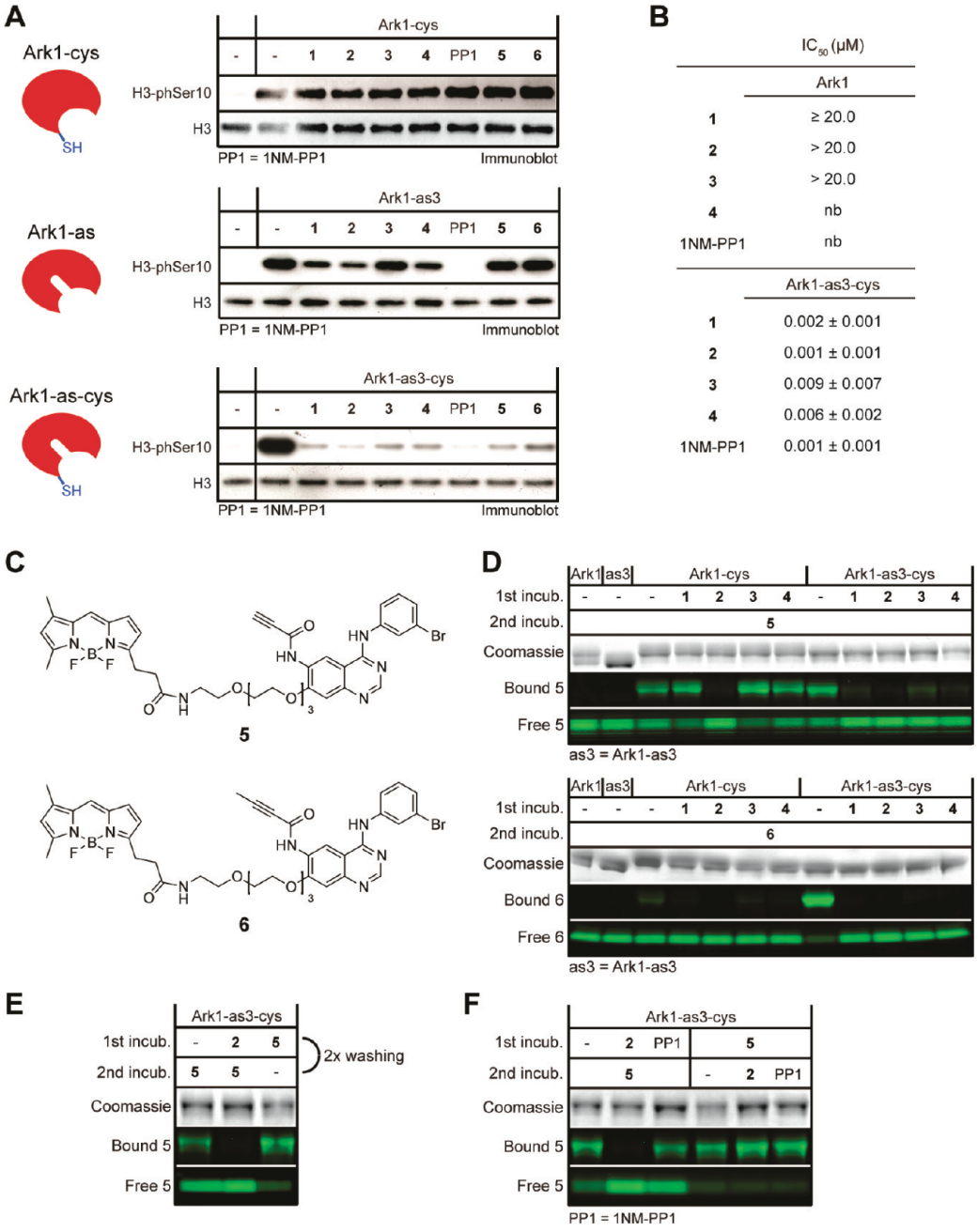

Figure 2. Compounds **1**−**4** specifically inhibit Ark1-as3-cys in biochemical assays. (A) Kinase assays with recombinant Ark1-cys (upper panel), Ark1-as3 (middle panel), and Ark1-as3-cys (lower panel), each incubated with the indicated compounds at 5 μM concentration prior to the addition of the substrate (histone H3). The reaction mixtures were separated by SDS-PAGE and immunoblotted with a phospho-specific antibody against Ser10 in histone H3 (H3-phSer10). Immunoblotting for histone H3 served as loading control. (B) IC_{50} values for the indicated compounds with wild type Ark1 or Ark1-as3-cys (see Supplementary Table 1 for full information). nb, non binding (no inhibitory effect at 50 μM). (C) Chemical structures of compounds **5** and **6**. (D) Recombinantly produced versions of Ark1 were preincubated with inhibitors for 5 min (1st incub.) followed by incubation with probes **5** (upper panel) or **6** (lower panel) for 5 min (2nd incub.). Reaction mixtures were separated by SDS-PAGE. Ark1 was detected by Coomassie staining. The amount of fluorescent compound comigrating with Ark1 ("Bound") or present in the running front of the SDS gel ("Free"), respectively, are shown. (E) Recombinantly produced Ark1-as3-cys was bound to beads, incubated for 5 min with **2** or **5** (1st incub.), washed twice, and incubated with **5**, as indicated, for another 5 min (2nd incub.). The reaction mixtures were analyzed as in panel D. (F) Recombinantly produced Ark1-as3-cys was incubated with the indicated compounds and analyzed as in panel D.

Ark1-as3-cys and to a much weaker extent to Ark1-cys, but not to Ark1 or Ark1-as3 (Figure 2D), highlighting the requirement of orthogonal filters for efficient targeting by the probe molecules. Binding of **6** to Ark1-as3-cys could be competed for by preincubation with **1**−**4**, indicating that all of these compounds specifically bind the engineered Cys173. In contrast to **6**, **5** showed equally strong binding to Ark1-cys and Ark1-as3-cys, and binding to Ark1-cys could be competed for by **2**, but not by **1**, **3**, or **4** (Figure 2D). This indicates that the most active compound **2**, which carries a propiolamide as the reactive group, covalently binds Ark1-cys in addition to Ark1-as3-cys. However, neither **2** nor **5** inhibited Ark1-cys in our biochemical assay (Figure 2A), confirming that presence of only one of the selectivity filters is insufficient for functionality

dx.doi.org/10.1021/cb200465c | ACS Chem. Biol. 2012, 7, 723−731

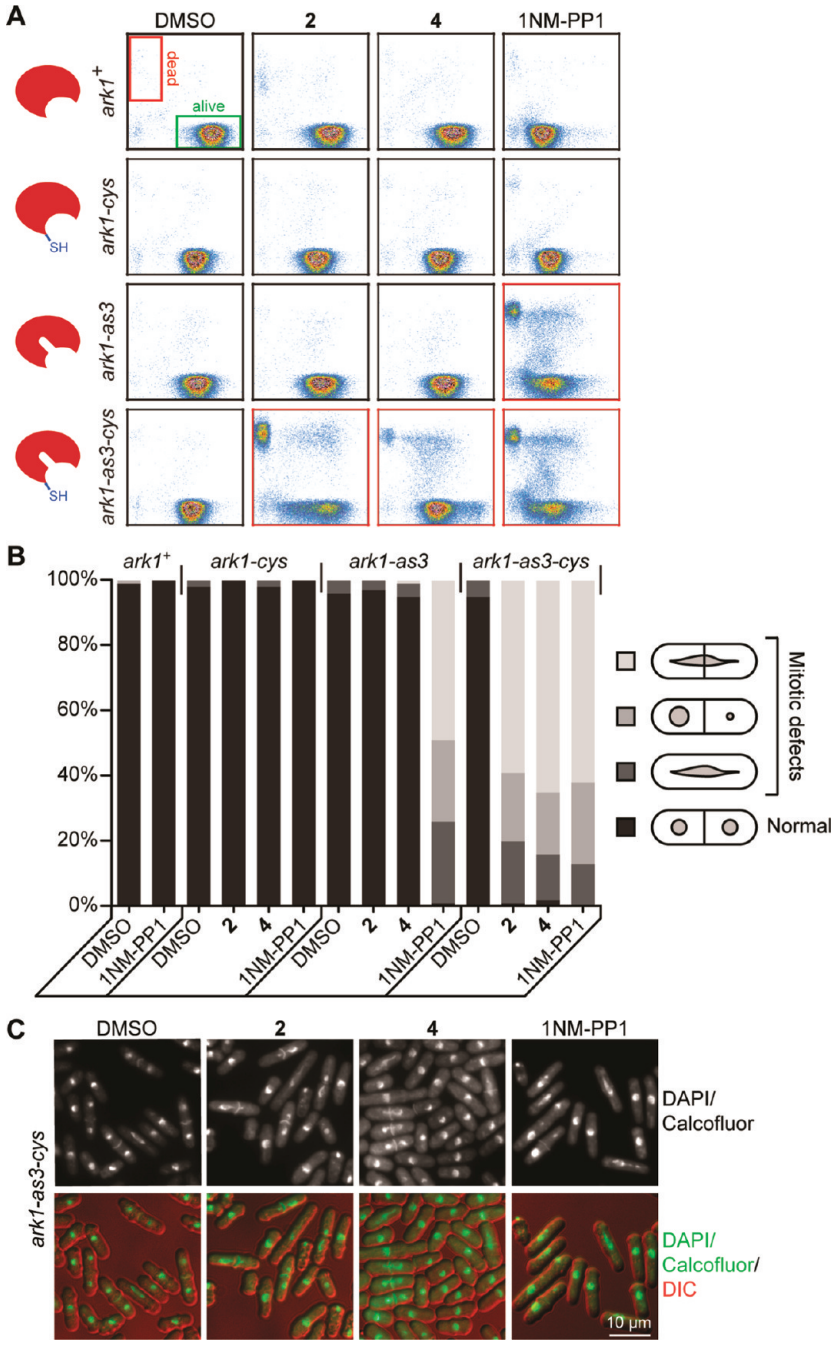

Figure 3. Compound **2** and **4** impair growth of *ark1-as3-cys*-expressing cells. (A) Cells in logarithmic growth phase expressing *ark1+*, *ark1-cys*, *ark1-as3*, or *ark1-as3-cys* were grown for 4 h in the presence of the indicated compounds at 5 μM concentration and stained with "Yeast viability kit" (Partec), and 50,000 cells of each treatment were measured in a flow cytometer. Viable cells cluster in the lower right (green box), and dead cells in the upper left (red box) of the scatter plot. Combinations of strain and compound that showed an increase in dead cells are marked with a red box. (B) Cells in logarithmic growth phase expressing *ark1+*, *ark1-cys*, *ark1-as3*, or *ark1-as3-cys* were grown for 2 h in the presence of the indicated compounds at 5 μM concentration, fixed with methanol, and stained with DAPI to visualize DNA and Calcofluor to visualize the cell wall. DNA segregation defects of late mitotic cells were scored as shown in the legend. Around 100 mitotic cells were analyzed for each condition. (C) Example pictures of *ark1-as3-cys*-expressing cells treated with the indicated inhibitors from the experiment shown in B.

of the probe. To exclude that reversible, rather than irreversible, binding of the nonfluorescent compounds lead to the reduced binding of **5** or **6**, we performed the assay with Ark1-as3-cys coupled to beads and stringently washed the beads after addition of **2** and before addition of **5** (Figure 2E). Compound **2** still competed for binding of **5** in this assay, indicating that not only **5** but also **2** bound covalently. In addition, unlike preincubation with **2**, preincubation of Ark1-as3-cys with the reversible inhibitor 1NM-PP1 did not prevent binding of **5** (Figure 2F). When **5** was added before **2**, compound **2** was unable to compete out **5** (Figure 2F). A similar result was obtained for **6** (Supplementary Figure 1B). We conclude that compounds **1**−**6** covalently bind the engineered Cys173 and that efficient binding depends on both selectivity filters.

Cellular Characterization of Functional Probes. In order to test the effect of these probes in cells, homologous

dx.doi.org/10.1021/cb200465c | *ACS Chem. Biol.* 2012, 7, 723−731

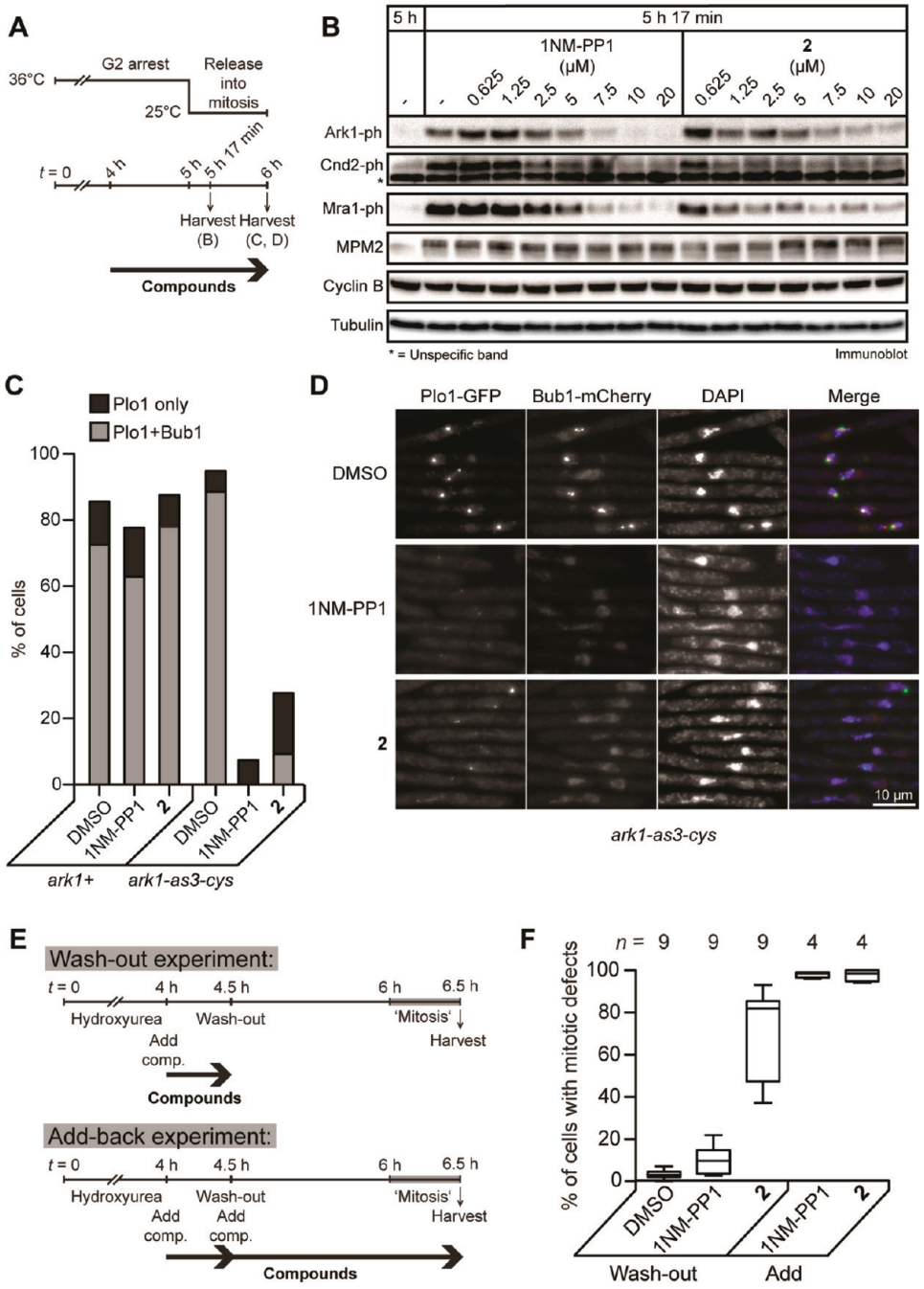

Figure 4. Compound **2** impairs the activity of Ark1-as3-cys in cells in an irreversible manner. (A) Schematic of the experiments shown in panels B, C, and D. Cells with the temperature-sensitive *cdc25-22* mutation were arrested prior to mitosis (in G2 phase) by culturing them for 5 h at 36 °C (restrictive temperature). During the last 1 h of the arrest, 1NM-PP1, **2**, or the solvent DMSO was added, and the cells were released synchronously into mitosis by shifting the culture to 25 °C. At the indicated points in time, cells were harvested for immunoblotting (B) or microscopic analysis (C, D). (B) Immunoblot of whole cell extracts at the time point of release into mitosis (5 h) and 17 min after the release (5 h 17 min), when cells had reached mitosis. Shown are the Ark1-specific phosphorylations on Ark1-Thr244 (Ark1-ph[21,22]), condensin subunit Cnd2-S5 (Cnd2-ph[23,24]), and Mra1-S9 (Mra1-ph[23]). The asterisk marks a cross-reacting band in the Cnd2 immunoblot. Presence of the MPM2 phosphoepitope[26] and cyclin B (fission yeast Cdc13[25]) indicates that the inhibitor-treated cells were in mitosis. Tubulin serves as loading control. (C) Bub1-mCherry and Plo1-GFP in *cdc25-22 cut7-446* cells were visualized by microscopy in cells harvested 1 h after release of the culture into mitosis. Bub1 is a spindle assembly checkpoint protein that localizes to kinetochores when the checkpoint is active.[36] Plo1 localizes to spindle pole bodies during early mitosis.[30] Pictures were scored for the presence of a localized Plo1-signal only or of both a localized Plo1- and Bub1-signal. In one set of experiments, cells expressed wild type *ark1+*, in the other *ark1-as3-cys*. More than 100 cells were analyzed for each condition. (D) Example pictures of *ark1-as3-cys* cells scored in panel C. Shown are the Plo1-GFP signal (green in the merged picture), the Bub1-mCherry signal (red in the merged picture), and DNA stained with DAPI (blue in the merged picture). (E) Schematic of wash-out (upper part) and add-back experiments (lower part) shown in panel F. Cells expressing *ark1-as3-cys* were arrested in S phase by culturing them for 5 h in hydroxyurea-containing medium. In the last 30 min of the incubation, 1NM-PP1, **2**, or DMSO was added and afterward washed out together with the hydroxyurea. Cells were then cultured either in the presence (add-back) or absence (wash-out) of 1NM-PP1 and **2** until harvesting shortly after mitosis. (F) The experiments outlined in E were performed multiple (*n*) times, and mitotic defects were scored as in Figure 3B. More than 100 cells were analyzed in each experiment for each condition. The lines in the

dx.doi.org/10.1021/cb200465c | *ACS Chem. Biol.* 2012, 7, 723–731

Figure 4. continued

box-whisker-plot indicate the minimum and maximum value for the percentage of cells with mitotic defects obtained in any of the *n* experiments, as well as the median and 25th and 75th quartile.

recombination was used to replace endogenous fission yeast Aurora (Ark1) with the modified alleles of the kinase. Similar to Ark1-as3,[16] both Ark1-cys and Ark1-as3-cys were able to functionally replace wild type Ark1, as cells expressing these kinase versions did not exhibit any overt defects during mitosis in the absence of inhibitor (Figure 3A,B). We incubated yeast cells expressing the different variants of Ark1 with **1**−**4** or 1NM-PP1 and assessed cell viability by flow cytometry (Figure 3A, Supplementary Figure 3). Ark1 is essential for cell viability,[20] and inhibition of the kinase therefore results in an accumulation of dead cells. As expected, treatment of *ark1-as3* cells with 5 μM 1NM-PP1 caused cell death, and a similar outcome was observed when using *ark1-as3-cys* cells. Interestingly, treatment with **2** or **4** at 5 μM specifically impaired viability of *ark1-as3-cys* cells, but not of *ark1+*, *ark1-as3*, or *ark1-cys* cells, indicating that both selectivity filters are needed for efficient inhibition by these molecules in cells. Compounds **1** and **3** at 5 μM did not affect viability of *ark1-as3-cys* cells (Supplementary Figure 3A). Compound **4** was less efficient in this assay when compared with **2** (Figure 3A), but its inhibitory effect on *ark1-as3-cys* cells could be enhanced by increasing the concentration to 50 μM (Supplementary Figure 3B). This indicates that the nature of the electrophile is important for efficient Ark1-as3-cys inhibition in cells. Whereas incubation of wild type yeast cells with a high concentration (50 μM) of 1NM-PP1 caused toxicity, **2** and **4** were tolerated at concentrations up to 50 μM (Supplementary Figure 3B). Hence, the range between efficient inhibition in cells and onset of toxicity is larger for **2** than for 1NM-PP1, indicating that the irreversible inhibitor may be more specific. In order to confirm that cell death was caused by inhibition of Ark1, we assessed the cellular phenotypes after treatment with the compounds. Inhibition of Ark1 leads to severe DNA segregation defects in mitosis, as exemplified by the phenotype of *ark1-as3* cells treated with 1NM-PP1 (Figure 3B,C).[16,20] Similar defects were observed in *ark1-as3-cys* cells upon treatment with **2** or **4**. In contrast, *ark1+*, *ark1-cys*, and *ark1-as3* cells did not show any obvious phenotype when treated with **2** or **4**, highlighting the selective inhibition of Ark1-as3-cys (Figure 3B,C).

To demonstrate Ark1 inhibition on the molecular level and to compare the potency of **2** and 1NM-PP1 in cells, we arrested *ark1-as3-cys* cells just prior to mitosis, added **2** or 1NM-PP1, and released cells into mitosis in the presence of these compounds (Figure 4A). Ark1-dependent phosphorylation sites in Ark1 itself[21,22] as well as in Cnd2[23,24] and Mra1[23] were phosphorylated in control-treated mitotic cells, but phosphorylation was strongly reduced in a concentration-dependent manner in cells treated with 1NM-PP1 or **2**, with both compounds showing a similar effect (Figure 4B). The presence of cyclin B (fission yeast Cdc13[25]) and of the MPM2 phosphoepitope[26] (Figure 4B) confirmed that the inhibitor-treated cells were still in mitosis and excluded that loss of phosphorylation on Ark1, Cnd2, and Mra1 was a secondary consequence of mitotic exit. This confirms that **2** inhibits the enzymatic activity of Ark1-as3-cys in cells. To further assess functional impairment of Ark1, we assayed the activity of the spindle assembly checkpoint (SAC), a cellular surveillance pathway that requires Ark1 activity.[27] The SAC was activated by a mutation in Kinesin-5 (*cut7-446*[28,29]) and the percentage of cells in mitosis was analyzed by localization of Plo1 (Figure 4C,D), which targets to spindle pole bodies specifically during mitosis.[30] Both 1NM-PP1 and **2** shortened the SAC-mediated mitotic delay in *ark1-as3-cys*-expressing cells, but not in cells expressing wild type *ark1* (Figure 4C,D), indicating that the compounds induced a SAC failure by inhibiting Ark1-as3-cys rather than through an unexpected off-target effect. Localization of the spindle assembly checkpoint protein Bub1 was lost after treatment of *ark1-as3-cys* cells with 1NM-PP1 or **2** (Figure 4C,D), presumably as a consequence of exit from mitosis.[27] The Bub1 signal persisted in *ark1+* cells treated with 1NM-PP1 or **2** (Figure 4C, Supplementary Figure 4), corroborating that these compounds do not show unexpected effects in mitosis.

Covalent inhibitors often bind irreversibly. To test whether inhibition of Ark1-as3-cys by **2** in cells is irreversible, we performed a wash-out experiment: *ark1-as3-cys* cells were arrested in S phase using hydroxyurea and treated with **2** or 1NM-PP1 for 30 min. Hydroxyurea and compound were then washed out, and cells were allowed to undergo G2 phase and enter mitosis in compound-free medium (Figure 4E). As a control, the compound was readded just after the wash-out (Figure 4E). DNA segregation defects in late mitosis were scored to assess the degree of Ark1 inhibition (Figure 4F). Whereas transient treatment with 1NM-PP1 during S phase caused hardly any DNA segregation defect in mitosis, transient treatment with **2** led to considerable defects in DNA segregation. This response was somewhat variable, and the number of cells with DNA segregation defects was not quite as high as after add-back of 1NM-PP1 or **2** (Figure 4F). Possible causes for this variable response could be (i) incomplete inhibition because the 30 min incubation was not long enough for covalent binding to all Ark1-as3-cys present in the cells, (ii) resynthesis of Ark1-as3-cys after the inhibitors had been washed out, or (iii) dissociation of the inhibitor with a slow off-rate in the considerable time span between inhibitor treatment and mitosis (1.5−2 h). At present, we cannot distinguish between these possibilities. Nevertheless, the more pronounced mitotic defects seen after transient treatment with **2** compared to transient treatment with 1NM-PP1 (Figure 4F) suggest that a considerable fraction of Ark1-as3-cys had become inhibited irreversibly.

Conclusion. Kinase inhibitors have proven powerful tools to dissect kinase function in cellular systems. Most kinase inhibitors however target the ATP binding site of the catalytic domain, which is highly conserved across all protein kinases, thus making it difficult to achieve high levels of selectivity needed for chemical biology research. Here we report on the use of a chemical-genetic approach, which is based on two selectivity filters for generating an orthogonal covalent kinase inhibitor pair for the Aurora kinase Ark1 in fission yeast. The inhibition of analogue-sensitive Ark1-as3-cys in cells was dependent on the nature of the electrophile present at the 6-position of the probes' quinazoline core. In many applications covalent inhibitors are superior in potency and ligand-target residence times when compared to reversible binders.[7] In order to achieve suitably high selectivity for covalent binders in biologically relevant systems, the reactivity and spatial position-

dx.doi.org/10.1021/cb200465c | *ACS Chem. Biol.* 2012, 7, 723−731

ing of the electrophiles must be tailored to the corresponding nucleophile in the target protein of interest. Among the tested compounds equipped with various electrophiles, **2** was the most potent entity and showed efficient and largely irreversible inhibition in cells while exhibiting no detectable toxicity, even at very high concentrations. Our results indicate that the combination of two selectivity filters increases specificity and highlights the importance for a given covalent probe to properly bind to the desired target in an initially reversible step to allow for residence time that is sufficient for covalent bond formation. Based on our and previous work,[7,11,18,31] we expect that this targeted design strategy can be extended to other kinases or to Aurora kinases from different organisms to make them susceptible to irreversible inhibitors. Such inhibitors can also act as scaffolds to develop activity-based probes,[32] which provide additional functionality.

METHODS

Compounds and Chemicals. Compounds **1**−**4** were prepared as described previously.[33] The scheme for synthesis of **5** and **6** is shown in Supplementary Figure 5. Anhydrous solvents were purchased from Acros Organics and Fluka. Other chemicals were purchased from Alfa Aesar, Fluka, and Sigma Aldrich and were used as received.

Analytical Data. ^{1}H and ^{13}C NMR spectra were recorded on a Varian Mercury 400, Bruker DRX 500 or Varian Inova 600 spectrometer. The spectra refer to the residual solvent signals: dimethylsulfoxide-d_6 (2.50 ppm) for ^{1}H and (39.52 ppm) for ^{13}C. Chemical shifts (δ) are given in parts per million (ppm), and the coupling constants (J) are reported in Hz. The following abbreviations are used: s = singlet, d = doublet, dd = doublet of doublet, ddd = doublet of doublet of doublet, t = triplet, td = triplet of doublets, dt = doublet of triplets, q = quartet, qd = quartet of doublet, qn = quintet, bs = broad singlet, m = multiplet. LC−MS spectra were obtained on a LTQ Orbitrap (high resolution mass spectrometer from Thermo Electron) coupled to an "Accela" HPLC System (consisting of Accela pump, Accela autosampler and Accela PDA detector) supplied with a "Hypersil GOLD" column (50 mm × 1 mm, 1.9 μm particle size) from Thermo Electron. Analytical TLC was carried out on Merck 60 F_{245} aluminum-backed silica gel plates. Preparative HPLC was carried out on the final compounds using a Varian Prostar with UV-detector (Model 340) and a VP 25-21 Nucleodur (C18 Gravity, 5 μm) column (serial no. 2105150).

*3-(1-((6-Amino-4-((3-bromophenyl)amino)quinazolin-7-yl)oxy)-12-oxo-3,6,9-trioxa-11-azatetradecan-14-yl)-5,5-difluoro-7,9-dimethyl-5H-dipyrrolo[1,2-c:2′,1′-f][1,3,2]diazaborinin-4-ium-5-uide (**vi**).* 7-(2-(2-(2-(2-Aminoethoxy)ethoxy)ethoxy)ethoxy)-N^4-(3-bromophenyl)quinazoline-4,6-diamine (**v**) (prepared as previously described[11]) (0.050 g, 0.09 mmol), 4,4-difluoro-5,7-dimethyl-4-bora-3a,4a-diaza-*s*-indacene-3-propionic acid, succinimidyl ester (0.038 g, 0.09 mmol), and diisopropylethylamine (20 μL, 0.11 mmol) were added in DMF (2 mL) and stirred at RT for 2 h. The reaction mixture was poured into water and extracted with EtOAc (4 × 100 mL). The organic phase was dried with Na_2SO_4 and concentrated under high vacuum. The crude product was purified by preparative HPLC to furnish 0.054 g (54%) of **vi** as an orange solid. ^{1}H NMR (400 MHz, DMSO-d_6): 9.45 (br s, 1H), 8.40 (s, 1H), 8.22 (s, 1H), 8.03 (t, J = 5.5 Hz, 1H), 7.86 (d, J = 8.2 Hz, 1H), 7.67 (s, 1H), 7.46 (s, 1H), 7.30 (t, J = 8.1 Hz, 1H), 7.21 (d, J = 7.9 Hz, 1H), 7.12 (s, 1H), 7.07 (d, J = 4.0 Hz, 1H), 6.34 (d, J = 4.0 Hz, 1H), 6.28 (s, 1H), 5.35 (br s, 2H), 4.28 (t, J = 4.0 Hz, 2H), 3.86 (t, J = 4.3 Hz, 2H), 3.67−3.62 (m, 2H), 3.59−3.49 (m, 6H), 3.38−3.29 (m, 2H), 3.41 (t, J = 5.8 Hz, 2H), 3.26−3.17 (m, 2H), 3.07 (t, J = 7.7 Hz, 2H), 2.45 (s, 3H), 2.24 (s, 3H). ^{13}C NMR (101 MHz, DMSO-d_6): 170.95, 162.39, 159.11, 157.74, 155.11, 151.91, 150.15, 144.07, 142.00, 138.57, 134.43, 132.97, 130.29, 128.93, 125.35, 124.93, 123.28, 121.20, 120.25, 119.90, 116.60, 110.59, 106.43, 101.13, 70.03, 69.86, 69.77, 69.61, 69.13, 68.70, 68.04, 38.63, 33.66, 24.01, 14.53, 11.02. HRMS (ESI-MS): calcd 780.24864 and 782.24660 for $C_{36}H_{42}{}^{79}BrBN_7O_5F_2$ [M + H$^+$] and $C_{36}H_{42}{}^{81}BrBN_7O_5F_2$ [M + H$^+$]; found 780.25022 and 782.24804.

*3-(1-((4-((3-Bromophenyl)amino)-6-propiolamidoquinazolin-7-yl)oxy)-12-oxo-3,6,9-trioxa-11-azatetradecan-14-yl)-5,5-difluoro-7,9-dimethyl-5H-dipyrrolo[1,2-c:2′,1′-f][1,3,2]diazaborinin-4-ium-5-uide (**5**).* Propiolic acid (6.7 μL, 0.10 mmol) and EDCI·HCl (0.020 g, 0.10 mmol) were stirred in DMF (4 mL) at 0 °C for 0.5 h. 3-(1-((6-Amino-4-((3-bromophenyl)amino)quinazolin-7-yl)oxy)-12-oxo-3,6,9-trioxa-11-azatetradecan-14-yl)-5,5-difluoro-7,9-dimethyl-5*H*-dipyrrolo-[1,2-*c*:2′,1′-*f*][1,3,2]diazaborinin-4-ium-5-uide (0.028 g, 0.04 mmol) was added, and the reaction mixture was stirred overnight at RT. The reaction mixture was then concentrated under high vacuum to 1 mL and poured into water. The resulted solution was then extracted with EtOAc (2 × 200 mL), and the EtOAc layer was washed with brine and dried over Na_2SO_4. Solvent was removed under high vacuum, and the resulted crude product was purified by preparative HPLC to give 0.002 g (7%) of **5** as an orange solid. HRMS (ESI-MS): calcd 832.24356 and 834.24151 for $C_{39}H_{42}{}^{79}BrBN_7O_6F_2$ [M + H$^+$] and $C_{39}H_{42}{}^{81}BrBN_7O_6F_2$ [M + H$^+$]; found 832.24455 and 834.2461.

*3-(1-((4-((3-Bromophenyl)amino)-6-(but-2-ynamido)quinazolin-7-yl)oxy)-12-oxo-3,6,9-trioxa-11-azatetradecan-14-yl)-5,5-difluoro-7,9-dimethyl-5H-dipyrrolo[1,2-c:2′,1′-f][1,3,2]diazaborinin-4-ium-5-uide (**6**).* 2-Butynoic acid (0.018 g, 0.21 mmol) and EDCI·HCl (0.034 g, 0.18 mmol) were stirred in DMF (1 mL) at 0 °C for 0.5 h. 3-(1-((6-Amino-4-((3-bromophenyl)amino)quinazolin-7-yl)oxy)-12-oxo-3,6,9-trioxa-11-azatetradecan-14-yl)-5,5-difluoro-7,9-dimethyl-5*H*-dipyrrolo-[1,2-*c*:2′,1′-*f*][1,3,2]diazaborinin-4-ium-5-uide (0.008 g, 0.01 mmol) was added, and the reaction mixture was stirred overnight at RT. The reaction mixture was concentrated under high vacuum, poured into water, and extracted with EtOAc (2 × 100 mL). The EtOAc layer was washed with brine and dried over Na_2SO_4. The solvent was removed under high vacuum, and the resulted crude product was purified by preparative HPLC to yield 0.001 g (12%) of **6** as an orange solid. HRMS (ESI-MS): calcd 846.25921 and 848.25716 for $C_{40}H_{44}{}^{79}BrBN_7O_6F_2$ [M + H$^+$] and $C_{40}H_{44}{}^{81}BrBN_7O_6F_2$ [M + H$^+$]; found 846.25991 and 848.25806.

Yeast Strains. Figure 3: *JY333 h- leu1 ade6-M216*; *SI205 h- leu1 ade6-M216 hygR≪ark1-cys(E173C)*; *SI239 h- leu1 ade6-M216 hygR≪ark1-as3*; *SI240 h- leu1 ade6-M216 hygR≪ark1-as3-cys*. Figure 4B: SI284″ *h- hygR≪ark1-as3-cys plo1+-GFP≪kanR cdc25-22*. Figure 4C,D: SM676 *h? hygR≪ark1-as3-cys plo1+-GFP≪kanR bub1+-mCherry≪natR cdc25-22 cut7-446*; *SP017 h? ade6-M216 plo1+-GFP≪kanR bub1+-mCherry≪natR cdc25-22 cut7−446*. Figure 4E,F: SI240 *h- leu1 ade6-M216 hygR≪ark1-as3-cys*.

The *ark1-cys and ark1-as3-cys* alleles were generated by PCR-based mutagenesis of Glu173 to Cys and reintegration into the endogenous locus. Sequence analysis revealed that ARG135 of *ark1-as3-cys* was in addition inadvertently changed to GLN. All other mutant alleles have been described previously.[16,28,34]

Cell Growth. *Schizosaccharomyces pombe* cells were cultured in rich medium (YEA) at 30 °C (Figures 3 and 4E,F) or in case of strains containing the temperature-sensitive *cdc25-22* allele at 25 °C (permissive temperature) and 36 °C (restrictive temperature) (Figure 4A−D).

Antibodies. The following antibodies were used: mouse monoclonal against histone H3 (05-499, Upstate Biotechnology), rabbit polyclonal against histone H3-S10ph (06-570, Upstate Biotechnology), rabbit monoclonal against Ark1-T244ph (2914S, Cell Signaling/NEB), mouse monoclonal against α-tubulin (T5168, Sigma), cyclin B (Cdc13) (NB200-576, Novus/Acris), and MPM2 (GTX14581, Acris/GeneTex). Anti-Cnd2-S5ph was raised in rabbit against the following peptide MKRA(Sph)LGGHAPEDC, and the serum was affinity purified. Anti-Mra1-S9ph was raised in rabbit against the following peptide TYSKRK(Sph)RGSLEVSC, and the serum was affinity purified. As secondary antibodies HRPO-coupled goat anti-mouse IgG (115-035-003, Dianova) and goat anti-rabbit IgG (111-035-003, Dianova) were used.

Protein Extraction. Cell pellets from 5 × 10^7 cells were resuspended in 1 mL of ice-cold 20% (v/v) TCA and pelleted by centrifugation (1000*g*, 2 min, RT). Cells were washed with 1 mL of 1

M Tris and pelleted again by centrifugation. The cell pellet was resuspended in 200 μL of 2x SDS sample buffer (125 mM Tris pH 6.8, 4% (w/v) SDS, 20% (v/v) glycerol, 200 mM DTT, 0.02% (w/v) bromophenol blue) and boiled at 95 °C for 10 min. Glass beads (500 μm) were added, and the mixture was subjected three times to 40 s of shaking in a FastPrep machine (FP120, Qbiogene). A hole was made in the bottom of the tube, and the cell extract was eluted into a new reaction tube by centrifugation (1000*g*, 1 min, RT) thereby separating the extract from the glass beads. The resulting samples were boiled again at 95 °C for 10 min and centrifuged (16000*g*, 10 min, RT) in order to pellet the cell debris. Samples were stored at −20 °C until loading on SDS-polyacrylamide gels.

Fixation and Microscopy of *Schizosaccharomyces pombe* Cells. An aliquot of the cultures was fixed in −20 °C methanol. After washing once with PEM (100 mM PIPES pH 6.9, 1 mM EGTA, and 1 mM $MgSO_4$)/methanol and once with PEM, DNA was stained with 1 μg/mL DAPI (4′,6-diamidino-2-phenylindole; Sigma-Aldrich). Images were acquired on a Zeiss AxioImager microscope coupled to a CCD (charged-coupled device) camera and processed with MetaMorph 7.6.0 software (Molecular Devices Corporation). Typically, a Z-stack of about 3 μm thickness, with single planes spaced by 0.3 μm, was acquired and subsequently projected to a single image. Shown in Figure 3C are color-combined pictures of single planes of the DAPI Z-stack (blue channel) and the single picture taken with differential interference contrast (DIC) (red channel). In Figure 4 maximum intensity projections of the GFP Z-stack (green channel) and the mCherry Z-stack (red channel) with single plains of the DAPI Z-stack (blue channel) are shown.

Cell Synchronization by *cdc25-22* Arrest-Release. Cells were arrested prior to mitosis by shifting the culture to 36 °C (restrictive temperature of the *cdc25-22* mutant) for 4 h and then treated for 60 min either with 10 μM 1NM-PP1 ((4-amino-1-*tert*-butyl-3-(1′-naphthylmethyl)pyrazolo[3,4-*d*]pyrimidine; Toronto Research Chemicals), 10 μM **2**, or the same amount of DMSO at 36 °C. Cells were released from the *cdc25-22* arrest by reducing the temperature back to 25 °C in an ice−water bath and were grown subsequently at 25 °C until cell harvest. At the indicated points in time 5×10^7 cells (protein extraction) and 1×10^7 cells (methanol fixation) were harvested by centrifugation (3000*g*, 1 min, RT).

Flow Cytometry. Cells were cultured at 30 °C for 4 h in the presence of the indicated compounds. About 4×10^6 cells were stained with "Cell Viability Kit" (Partec) and measured in a flow cytometer (CyFlow SL, Partec).

Hydroxyurea Wash-out Experiment. Cells were grown in 10 mL of YEA to a concentration of 4×10^6 cells/mL, and 12 mM hydroxyurea (Sigma) was added to the culture. After 4 h, 5 or 10 μM 1NM-PP1, 10 μM **2**, or an equal amount of the solvent DMSO was added for 30 min. To wash out hydroxyurea, cells were pelleted (1000*g*, 3 min, RT) and washed with 50 mL of fresh YEA for 2 min with thorough mixing. Washing was repeated twice. After the three washing steps, the cells were taken up in 10 mL of YEA and grown either in the presence or absence of 5 μM 1NM-PP1 or **2**. Two hours after washing out hydroxyurea, the cells were fixed with methanol for microscopic analysis.

Kinase Assay Using Histone H3 as Substrate. Ark1 wild type and mutant versions were purified as previously described,[23] and 100 ng of the different versions of Ark1/Pic1 was incubated for 10 min at 32 °C with the indicated compounds at 5 μM in a buffer containing 50 mM Tris-HCl pH 7.5, 100 mM NaCl, 20 mM $MgCl_2$, 1 mM DTT, 1 mM ATP. After this incubation, 1 μg of histone H3 protein (calf thymus, Roche) was added, and the mixture was incubated for 15 min at 32 °C before addition of SDS-sample buffer and boiling at 95 °C for 10 min.

Determination of IC_{50} and K_m. Experiments were carried out using a homogeneous time-resolved FRET (HTRF) assay (KinEase-STK from Cisbio) according to the manufacturer's instructions and as published previously.[35] Concentrations of ATP and substrate were set around their respective K_m values (Supplementary Table 2) for each tested kinase and mutant variant. Each determination was replicated at least three times and in duplicate.

Binding Assay with BODIPY-Labeled Compounds. Five hundred nanograms of wild type Ark1 or mutant versions (purified together with Pic1) was incubated with the indicated compounds at 5 μM in a buffer containing 50 mM Tris-HCl pH 6.8, 100 mM NaCl, 1 mM DTT, 20 mM $MgCl_2$ for 5 min at 32 °C; a second compound at 5 μM was added, and the mixture was incubated for an additional 5 min at 32 °C before addition of SDS-sample buffer and boiling at 95 °C for 10 min. Samples were separated on a 10% SDS-polyacrylamide gel, and fluorescence of **5** and **6** was detected by scanning the gel in a VersaDoc imaging system (BioRad; 530 BP filter and blue laser). As a loading control for Ark1, the gel was stained with Coomassie.

For the binding assay with wash-out of compounds, 4 μg of Ark1-as3-cys was bound to Ni-NTA agarose beads (Qiagen). After the first incubation with the indicated compounds at 5 μM, the Ni-NTA-coupled kinase was washed twice with a 10 times excess of buffer (50 mM Tris-HCl pH 6.8, 100 mM NaCl, 1 mM DTT, 20 mM $MgCl_2$) and then incubated with **5** at 5 μM concentration.

■ ASSOCIATED CONTENT

Ⓢ Supporting Information

This material is available free of charge *via* the Internet at http://pubs.acs.org.

■ AUTHOR INFORMATION

Corresponding Author

*E-mail: daniel.rauh@tu-dortmund.de; silke.hauf@tuebingen.mpg.de.

Author Contributions

[#]These authors contributed equally to this work.

■ ACKNOWLEDGMENTS

We thank E. Illgen for excellent technical support, S. Graf for help with immunoblotting, and J. Kamenz for generating the *bub1+-mCherry* strain. The work was supported by the German Federal Ministry for Education and Research through the German National Genome Research Network-Plus (NGFN-Plus) (Grant No. BMBF 01GS08104 to D.R.) and by the Max Planck Society. MSD, Bayer HealthCare, Merck-Serono and Bayer CropScience are thanked for financial support.

■ REFERENCES

(1) Manning, G., Plowman, G. D., Hunter, T., and Sudarsanam, S. (2002) Evolution of protein kinase signaling from yeast to man. *Trends Biochem. Sci. 27*, 514−520.

(2) Manning, G., Whyte, D. B., Martinez, R., Hunter, T., and Sudarsanam, S. (2002) The protein kinase complement of the human genome. *Science 298*, 1912−1934.

(3) Cohen, P. (2002) Protein kinases−the major drug targets of the twenty-first century? *Nat. Rev. Drug Discovery 1*, 309−315.

(4) Knight, Z. A., and Shokat, K. M. (2007) Chemical genetics: where genetics and pharmacology meet. *Cell 128*, 425−430.

(5) Rabiller, M., Getlik, M., Kluter, S., Richters, A., Tuckmantel, S., Simard, J. R., and Rauh, D. (2010) Proteus in the world of proteins: conformational changes in protein kinases. *Arch. Pharm. (Weinheim, Ger.) 343*, 193−206.

(6) Singh, J., Petter, R. C., Baillie, T. A., and Whitty, A. (2011) The resurgence of covalent drugs. *Nat. Rev. Drug Discovery 10*, 307−317.

(7) Copeland, R. A., Pompliano, D. L., and Meek, T. D. (2006) Drug-target residence time and its implications for lead optimization. *Nat. Rev. Drug Discovery 5*, 730−739.

(8) Garske, A. L., Peters, U., Cortesi, A. T., Perez, J. L., and Shokat, K. M. (2011) Chemical genetic strategy for targeting protein kinases based on covalent complementarity. *Proc. Natl. Acad. Sci. U.S.A. 108*, 15046−15052.

(9) Zhang, J., Yang, P. L., and Gray, N. S. (2009) Targeting cancer with small molecule kinase inhibitors. *Nat. Rev. Cancer 9*, 28−39.

(10) Wissner, A., and Mansour, T. S. (2008) The development of HKI-272 and related compounds for the treatment of cancer. *Arch. Pharm. (Weinheim, Ger.) 341*, 465−477.
(11) Blair, J., Rauh, D., Kung, C., Yun, C., Fan, Q., Rode, H., Zhang, C., Eck, M., Weiss, W., and Shokat, K. (2007) Structure-guided development of affinity probes for tyrosine kinases using chemical genetics. *Nat.Chem. Biol. 3*, 229−238.
(12) Poulikakos, P. I., Zhang, C., Bollag, G., Shokat, K. M., and Rosen, N. (2010) RAF inhibitors transactivate RAF dimers and ERK signalling in cells with wild-type BRAF. *Nature 464*, 427−430.
(13) Vader, G., and Lens, S. M. (2008) The Aurora kinase family in cell division and cancer. *Biochim. Biophys. Acta 1786*, 60−72.
(14) Ruchaud, S., Carmena, M., and Earnshaw, W. C. (2007) Chromosomal passengers: conducting cell division. *Nat. Rev. Mol. Cell Biol. 8*, 798−812.
(15) Janmaat, M. L., and Giaccone, G. (2003) The epidermal growth factor receptor pathway and its inhibition as anticancer therapy. *Drugs Today 39* (Suppl C), 61−80.
(16) Hauf, S., Biswas, A., Langegger, M., Kawashima, S. A., Tsukahara, T., and Watanabe, Y. (2007) Aurora controls sister kinetochore mono-orientation and homolog bi-orientation in meiosis-I. *EMBO J. 26*, 4475−4486.
(17) Bishop, A. C., Buzko, O., and Shokat, K. M. (2001) Magic bullets for protein kinases. *Trends Cell Biol. 11*, 167−172.
(18) Kluter, S., Simard, J. R., Rode, H. B., Grutter, C., Pawar, V., Raaijmakers, H. C., Barf, T. A., Rabiller, M., van Otterlo, W. A., and Rauh, D. (2010) Characterization of irreversible kinase inhibitors by directly detecting covalent bond formation: a tool for dissecting kinase drug resistance. *ChemBioChem 11*, 2557−2566.
(19) Smaill, J. B., Rewcastle, G. W., Loo, J. A., Greis, K. D., Chan, O. H., Reyner, E. L., Lipka, E., Showalter, H. D., Vincent, P. W., Elliott, W. L., and Denny, W. A. (2000) Tyrosine kinase inhibitors. 17. Irreversible inhibitors of the epidermal growth factor receptor: 4-(phenylamino)quinazoline- and 4-(phenylamino)pyrido[3,2-*d*]-pyrimidine-6-acrylamides bearing additional solubilizing functions. *J. Med. Chem. 43*, 1380−1397.
(20) Petersen, J., Paris, J., Willer, M., Philippe, M., and Hagan, I. M. (2001) The S. pombe aurora-related kinase Ark1 associates with mitotic structures in a stage dependent manner and is required for chromosome segregation. *J. Cell Sci. 114*, 4371−4384.
(21) Leverson, J. D., Huang, H. K., Forsburg, S. L., and Hunter, T. (2002) The Schizosaccharomyces pombe aurora-related kinase Ark1 interacts with the inner centromere protein Pic1 and mediates chromosome segregation and cytokinesis. *Mol. Biol. Cell 13*, 1132−1143.
(22) Yasui, Y., Urano, T., Kawajiri, A., Nagata, K., Tatsuka, M., Saya, H., Furukawa, K., Takahashi, T., Izawa, I., and Inagaki, M. (2004) Autophosphorylation of a newly identified site of Aurora-B is indispensable for cytokinesis. *J. Biol. Chem. 279*, 12997−13003.
(23) Koch, A., Krug, K., Pengelley, S., Macek, B., and Hauf, S. (2011) Mitotic substrates of the kinase aurora with roles in chromatin regulation identified through quantitative phosphoproteomics of fission yeast. *Sci. Signaling 4*, rs6.
(24) Tada, K., Susumu, H., Sakuno, T., and Watanabe, Y. (2011) Condensin association with histone H2A shapes mitotic chromosomes. *Nature 474*, 477−483.
(25) Moreno, S., Hayles, J., and Nurse, P. (1989) Regulation of p34cdc2 protein kinase during mitosis. *Cell 58*, 361−372.
(26) Davis, F. M., Tsao, T. Y., Fowler, S. K., and Rao, P. N. (1983) Monoclonal antibodies to mitotic cells. *Proc. Natl. Acad. Sci. U.S.A. 80*, 2926−2930.
(27) Petersen, J., and Hagan, I. M. (2003) S. pombe aurora kinase/survivin is required for chromosome condensation and the spindle checkpoint attachment response. *Curr. Biol. 13*, 590−597.
(28) Hagan, I., and Yanagida, M. (1990) Novel potential mitotic motor protein encoded by the fission yeast cut7+ gene. *Nature 347*, 563−566.
(29) Windecker, H., Langegger, M., Heinrich, S., and Hauf, S. (2009) Bub1 and Bub3 promote the conversion from monopolar to bipolar chromosome attachment independently of shugoshin. *EMBO Rep. 10*, 1022−1028.
(30) Mulvihill, D. P., Petersen, J., Ohkura, H., Glover, D. M., and Hagan, I. M. (1999) Plo1 kinase recruitment to the spindle pole body and its role in cell division in Schizosaccharomyces pombe. *Mol. Biol. Cell 10*, 2771−2785.
(31) Salomon, D., Zhang, C., Shokat, K. M., and Sessa, G. (2011) Sensitizing plant protein kinases to specific inhibition by ATP-competitive molecules. *Methods Mol. Biol. 779*, 185−197.
(32) Nomura, D. K., Dix, M. M., and Cravatt, B. F. (2010) Activity-based protein profiling for biochemical pathway discovery in cancer. *Nat. Rev. Cancer 10*, 630−638.
(33) Sos, M. L., Rode, H. B., Heynck, S., Peifer, M., Fischer, F., Kluter, S., Pawar, V. G., Reuter, C., Heuckmann, J. M., Weiss, J., Ruddigkeit, L., Rabiller, M., Koker, M., Simard, J. R., Getlik, M., Yuza, Y., Chen, T. H., Greulich, H., Thomas, R. K., and Rauh, D. (2010) Chemogenomic profiling provides insights into the limited activity of irreversible EGFR Inhibitors in tumor cells expressing the T790M EGFR resistance mutation. *Cancer Res. 70*, 868−874.
(34) Russell, P., and Nurse, P. (1986) cdc25+ functions as an inducer in the mitotic control of fission yeast. *Cell 45*, 145−153.
(35) Getlik, M., Grutter, C., Simard, J. R., Kluter, S., Rabiller, M., Rode, H. B., Robubi, A., and Rauh, D. (2009) Hybrid compound design to overcome the gatekeeper T338M mutation in cSrc. *J. Med. Chem. 52*, 3915−3926.
(36) Bernard, P., Hardwick, K., and Javerzat, J. P. (1998) Fission yeast bub1 is a mitotic centromere protein essential for the spindle checkpoint and the preservation of correct ploidy through mitosis. *J. Cell Biol. 143*, 1775−1787.